



ISSN NO. 2320-5407

Journal homepage: <http://www.journalijar.com>

INTERNATIONAL JOURNAL
OF ADVANCED RESEARCH

RESEARCH ARTICLE

Influence of limestone on physico-chemical properties of white portland cement pastes

A.M. El-Roudi, Basma A.A Balboul and M.A. Abdelzaher*

Chemistry Department, Faculty of Science, Minia University, Minia, Egypt.

Manuscript Info

Manuscript History:

Received: 14 April 2015
Final Accepted: 25 May 2015
Published Online: June 2015

Key words:

Ordinary White Portland Cement (OWPC), Limestone, XRF, XRD, FTIR, SEM, TGA/DTA

*Corresponding Author

M.A. Abdelzaher

Abstract

This paper aims to study physico-chemical properties of white Portland cement blended with 5-25 wt. % limestone filler. It was observed that limestone filler increases whiteness, Blaine and loss on ignition of dry blended cement powders increases with limestone content. Limestone filler increases setting times, free lime content, total porosity, decreases compressive strength, combined water content and bulk density of cement pastes due to the filling effect of limestone that replaces clinker and decreases the amount of hydration products. Portlandite was detected in limestone blended cement pastes hydrated for 7 days by XRD indicating the filler effect of limestone at early ages of hydration. Whereas, C3S was not detected in limestone blended cement pastes hydrated up to 90 days by XRD due to that limestone filler accelerates the rate of hydration of C3S. Calcium monocarboaluminate was detected by FTIR in cement pastes hydrated for 7 days this means that C3A reacts with CaCO_3 giving calcium monocarboaluminate hydrate. The absorption band of ettringite disappeared due to that SO_4^{2-} ions were probably replaced by CO_3^{2-} . The OH band of combined water, associates hexagonal hydrates and calcium hydroxide was shifted in FTIR spectra of cement pastes, demonstrating the accelerating effect of CaCO_3 on C3S hydration and formation of calcium carboaluminate hydrate. Relative weight losses that correspond to dehydration of C-S-H, ettringite and portlandite (calculated from TGA/DTA thermograms) prove the dilution effect of limestone filler. SEM micrographs of limestone blended cement pastes hydrated up to 90 days show that limestone filler alters the microstructure of hardened cement pastes. The morphology of calcium monocarboaluminate hydrate originally changes with progress of hydration.

Copy Right, IJAR, 2015., All rights reserved

INTRODUCTION

Addition of limestone filler to clinker may complete the fine fraction in the granulometric curve of cement without an increment on water demand, improves the cement packing and blocks the capillary pores. Hence, many researchers proved that addition of limestone to cement slightly decreases water demand [1-3], setting times and total porosity [1 and 4], whereas increases combined water content [1, 4 and 5] and compressive strength up to 15% of cement paste [1 and 2]. Limestone develops almost the same compressive strength as the corresponding pure cement [3]. Limestone filler increases rate of the hydration at early ages giving a high early strength [7 and 8]. Limestone reacts with aluminates and ferrite phases from cement to form monocarboaluminate [9-11]. It acts also as a nucleating sites for cement hydration products due to its high specific surface and incorporates into the calcium silicate hydrates C-S-H themselves [12 and 13] accelerating the hydration of clinker particles especially the C3S [6] improving early strength [14]. The C-S-H crystal size is diminished [15-17]. Limestone addition may lead to the formation of some calcium carboaluminate hydrate [6], and reduces the potential cementing material (dilution effect) causing a reduction of later strength [6, 7 and 18]. For severely aggressive environments, more important durability

problems reported in Portland limestone cements are susceptible to sulphate attack (especially, thaumasite formation) and chloride-ion diffusion depending on the level of addition [19 and 20]. In contrast, addition of limestone also slightly increases the water demand and total porosity of Portland cement pastes and decreases setting times as well as bulk density of Portland cement pastes [21].

Limestone filler influences the rate of hydration processes due to its modified nucleation possibility. The reaction mechanism of the Portland cement is altered [22]. Limestone filler reacts with C3A forming monocarboaluminates [11 and 23]. This in turn, stabilizes ettringite [23], i.e. delays or impedes the ettringite-monosulfoaluminate transformation [11]. Stabilization of ettringite leads to increase the total volume of the hydrated phase and decrease the porosity of cement pastes. The relative amount of hydrated phases C3A, portlandite and fixed sulfate ratio in dependence of changing carbonate ratios were calculated to explain how does limestone alter the mineralogy of hydrated cement pastes [24]. At the outset of limestone addition, very small changes in the calcium carbonate ratio lead to rapid consumption of monosulfoaluminate, while that of hemicarboaluminate increases rapidly. Sulfate released from monosulfoaluminate forms ettringite. As a result, portlandite contents decrease sharply from the original amount. Upon continued addition of limestone, hemicarboaluminate is progressively replaced by monocarboaluminate. Hence, portlandite liberated by limestone additions. Calculations of the specific volume of solids as a function of limestone addition suggest that the space-filling ability of the paste is optimized when the limestone content is adjusted to maximize the ettringite content. The effect of high limestone filler addition upon the rheological properties of cement pastes was studied. Addition of limestone filler improves the fine-particle packing and considerably enhances stability and workability of fresh concrete [10, 25 and 26], inhibits the induced bleeding of fresh high-strength concrete [10], as well as increases the density of paste matrix and interfacial transition zone in hardened concrete [4 and 27]. Addition of limestone filler increases total porosity of cement mortars. Moreover, intrinsic gas permeability, compressive and flexural strengths remain remarkably high. Drying shrinkage and mass loss are not impacted dramatically either [28]. Fine limestone filler complements the deficiency in fine particles of the particle size distribution of cement, which can enhance both the flow ability as well as stability of fresh concrete and fill in between the relatively coarser cement grains, reducing the water demand and enhance the packing density of high-performance concrete. The yield stress value and viscosity of cement paste decreased with limestone content [29]. Mortars with a high limestone content exhibit a more packed microstructure, which facilitates setting of cement and results in improved mortar strength [30].

The initial setting time of white cement paste was shorter whereas the early tensile and compressive strengths were greater for the white cement mortars than the gray cement mortars due to the high percentage of C3A content and much small C4AF content in the white cement. The later tensile and compressive strength were greater for the white cement mortars than the gray cement mortars due to the higher total percentage of the silicates (C3S + C2S) in the white cement. The relatively higher percentage of C3A in the white cement leads to higher early rate of hydration and strength gain of white cement concrete [31]. Considerable fraction of the aluminium is present as Al³⁺ guest-ions in the calcium silicate phases alite and belite [32 and 33]. During hydration of Portland cements in presence of gypsum, the principal hydration products of the calcium aluminate and aluminoferrite phases are the Aft and AFm phases ettringite ($\text{Ca}_6[\text{Al}(\text{OH})_6]_2(\text{SO}_4)_3 \cdot 16\text{H}_2\text{O}$) and monosulphate ($\text{Ca}_4[\text{Al}(\text{OH})_6]_2\text{SO}_4 \cdot 16\text{H}_2\text{O}$). A significant quantity of aluminium is incorporated in the calcium-silicate-hydrate C-S-H phase, where AlO₄ units take part in the tetrahedral chain structure of SiO₄ tetrahedra [34 and 35]. For C-S-H phases with high Ca/Si ratios, it has also been proposed that Al may be incorporated in the interlayer region of the C-S-H structure, potentially by substitution for interlayer Ca²⁺ ions, forming AlO₆ octahedra [36-38]. Considering the low Al₂O₃ content of Portland cements, it can be hard to identify the abovementioned aluminate phases, even though some of them are present in a crystalline form, since they may be present in quantities less than 1 wt.% of the hydrated Portland cement.

The potential of ²⁷Al MAS NMR in studies of Portland cements was demonstrated in a preliminary investigation of a white Portland cement [39], where the hydration of the calcium aluminate phase could be followed by the distinction of tetrahedrally and octahedrally coordinated Al species. Hydration of white Portland cement at different temperatures was studied by ²⁹Si and ²⁷Al spectroscopy. Monosulphoaluminate and C-S-H gel are formed during white cement hydration. White cement hydration generates a C-S-H gel in which the aluminium taken up forms bridge bonds and C-S-H gel chain length increases with temperature [40]. The microstructure of hardened pastes of 20% metakaolin blended white Portland cement have been studied using solid-state ²⁹Si and ²⁷Al MAS NMR spectroscopy and analytical TEM. Long-chain highly aluminous C-S-H, with most of the bridging sites occupied by Al³⁺ rather than Si⁴⁺ was formed in these cement pastes. Both the tobermorite/jennite

(T/J) and tobermorite/calcium hydroxide (T/CH) models of the nanostructure of C–S–H formed [41]. The inner product C–S–H generally had a fine scale, homogeneous morphology and the outer product C–S–H has both fine-fibrillar and foil-like morphologies in the water-activated paste [41 and 42]. Limestone reacts with C3A forming the hemicarboaluminate, $(C3A \cdot 0.5CaCO_3 \cdot 0.5Ca(OH)_2 \cdot 11.5H_2O)$ and forming of the monocarboaluminate phase $(C3A \cdot CaCO_3 \cdot 11H_2O)$. The formation of C4AH13 and C2AH8 is prohibited and the generation of C3AH6 is delayed in the early hydration process. Hemicarboaluminate is unstable and will be totally transformed within 24 hrs. to monocarboaluminate hydrate that exists stably once formed [43]. The influence of limestone on the hydration of gray Portland cement was well studied worldwide. In addition, there are little works studied the hydration characteristics of white Portland cement. In contrast, there is a lake of knowledge dealing with the role of limestone on the hydration of white Portland cement. The aim of this research is to study influence of limestone on the physico-chemical properties of white Portland cement.

Materials and Methods

Ordinary white Portland cement (OWPC) clinker, gypsum and white limestone filler used in this study were provided from Helwan Cement Co. ELMinya plant, Minia Governorate, Egypt. Five mix patches of limestone blended cement were prepared by partial replacement of OWPC with 5–25% limestone in presence of constant clinker/gypsum ratio of 0.95. Table (1) illustrates the mix composition of limestone blended cements in wt%. Table (2) illustrates the chemical composition wt % of ordinary white Portland cement (OWPC) limestone determined by XRF analysis. Table (3) illustrates the phase composition and lime saturation factor LSF of OWPC, wt % determined by to Bouge's calculations.

TABEL (1): Mix composition, wt.% of limestone blended cements

Mix	OWPC	Limestone	Total Mix.
C	100	0	100
L1	95	5	100
L2	90	10	100
L3	85	15	100
L4	80	20	100
L5	75	25	100

The water of consistency, initial and final setting times were determined using Vicat apparatus according to ASTM designations [44 and 45]. Cement pastes were hydrated with their corresponding water of consistency. Freshly prepared cement pastes were molded in stainless steel molds (2x2x2 cm) at about 100% relative humidity and 21 ± 2 °C demolded after 24 hrs. and cured up to 90 days in tap water. Bulk density was determined using Archimedes principle [46]. The compressive strength was measured using a manual compressive strength machine for a set of three cubes according to ASTM designation [47]. Free water content was determined using domestic microwave oven (Olympic electric model KOR-131G, 2450 MHz, 1000 W) [48].

The combined water content was determined using dried specimens after igniting in porcelain crucibles at 1000°C for 1 h. The total porosity of the hardened cement paste was calculated from the values of bulk density, free and total water contents as described elsewhere [49]. The free lime content of hardened cement pastes was determined according to [50]. X-ray fluorescence (XRF) and X-ray diffraction (XRD) analyses were carried out by Philips X-ray diffractometer PW 1370, Co. with Ni filtered $CuK\alpha$ radiation (1.5406Å). The Fourier transform infrared (FTIR) analysis was measured by spectrometer Perkin Elmer FTIR system Spectrum X in the range 400–4000 cm^{-1} with spectral resolution of 1 cm^{-1} . Scanning electron microscopy (SEM) was investigated using Jeol-Dsm 5400 LG apparatus.

TABEL (2): CHEMICAL COMPOSITION OF RAW MATERIALS BY XRF

Oxide	SiO ₂	Al ₂ O ₃	CaO	Fe ₂ O ₃	MgO	SO ₃	Na ₂ O	K ₂ O	Cl	LOI	Total
OWPC	22.07	3.00	68.41	0.14	0.31	2.84	0.03	0.06	0.02	2.35	99.23
Limestone	0.28	0.04	54.77	0.03	0.20	0.14	0.04	0.03	0.02	43.72	99.27

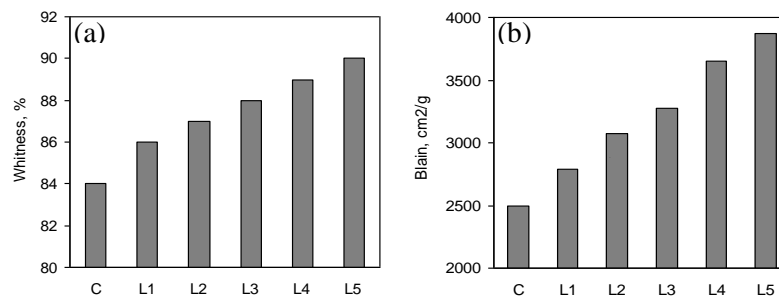
TABEL (3): PHASE COMPOSITION OF OWPC, WT % DETERMINED BY BOUGE'S CALCULATIONS

Phase	Content, wt %
C3S	75.66
β -C2S	8.95
C3A	7.70
C4AF	0.42
LSF	0.98

Results and Discussion

1. Whiteness and Blaine

Figure (1) illustrates the whiteness and Blaine of OWPC as well as limestone dry cement mixtures. It was observed that both whiteness and Blaine (cm^2/g) of dry cement powders increase with limestone content. This is regarded to the high whiteness as well as Blaine (cm^2/g) of limestone itself compared to white Portland cement. The whiteness values are 98.20% and 84.00% for limestone and white Portland cement respectively. The Blaine (cm^2/g) values are 6669 and 2500 for limestone and white Portland cement respectively.

FIGURE (1): (a) Whiteness, % and (b) Blaine, cm^2/g of OWPC and limestone dry cement mixtures

2. Setting

Figure (2) illustrates the initial and final setting times of OWPC and limestone dry cement mixtures. It was observed that both initial as well as final setting times of hydrated cement pastes elongate with limestone content. The retardation effect in case of limestone dry cement mixtures arises from that limestone grains coat around un-hydrated white Portland cement grains delaying its hydration reaction. Hence, the setting time elongates with increasing limestone filler content.

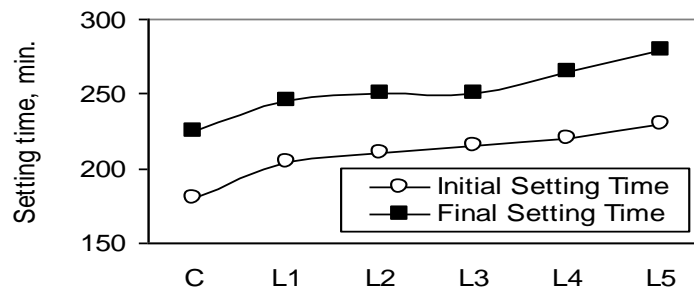


FIGURE (2): Initial and final setting times of OWPC and limestone blended cement pastess

3. Compressive Strength

Figure (3) illustrates the compressive strength of OWPC and limestone blended cement pastes. The compressive strength of cement pastes increases with curing time for all cement pastes as a result of the hydration of clinker phases and formation of further hydration products that fill some of pores in the cement paste. As the hydration proceeds, more hydration products and more cementing materials are formed leading to increase the compressive strength of cement pastes. This is mainly due to that the hydration products possess a large specific

volume than the un-hydrated cement. Therefore, the accumulation and compaction of these hydrated products give higher strength. The compressive strength of cement pastes decreases with limestone content due to dilation effect that decreases the amount of hydration products especially C–S–H which is the main binding component.

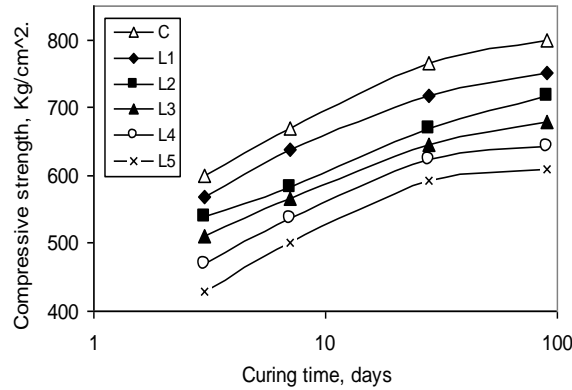


FIGURE (3): Compressive strength of OWPC and limestone blended cement pastes

4. Loss On Ignition (LOI)

Figure (4) illustrates the loss on ignition (LOI) of dry OWPC and limestone dry cement mixtures. It was observed that the ignition loss increases with limestone content because limestone decomposes at 900-1000 oC forming CaO and CO₂ with about 43.72 % weight loss.

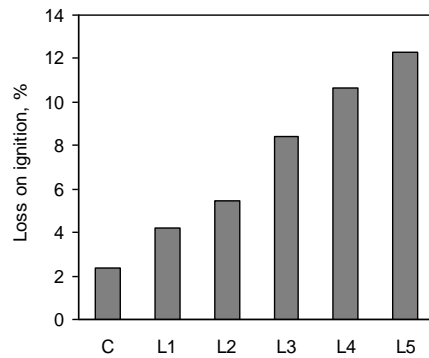


FIGURE (4): Loss on ignition of dry OWPC and limestone dry cement mixtures

5. Combined Water Content

Figure (5) illustrates the combined water content of OWPC and limestone blended cement pastes. The combined water content increases with curing time for all cement pastes as a result of the progress of hydration process and formation of additional hydration products. The combined water content decreases with limestone content due to limestone has no cementations properties. As recommended for a better evaluation of the hydration process, all the estimated contents and the water released from other hydrates were calculated with reference to the final ignited mass of the pastes at 1000 oC [51]. The actual combined water content of each cement pastes was corrected from the ignition loss of each dry cement mix as shown in figure (4).

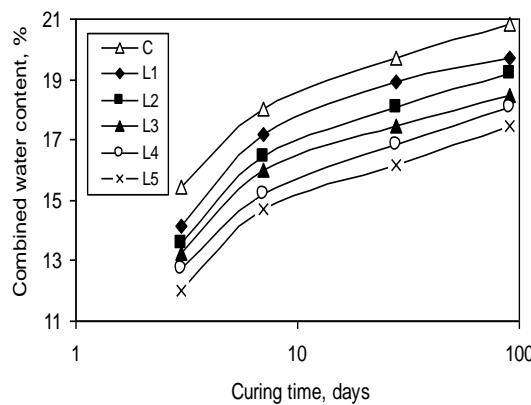


FIGURE (5): Combined water content of OWPC and limestone blended cement pastes

6. Bulk Density and Total Porosity

Figure (6) illustrates the bulk density and total porosity of OWPC and limestone blended cement pastes. The bulk density of cement pastes increases with curing time for all cement pastes as a result of the hydration of clinker phases and formation of further hydration products that fill some of pores in the cement paste. The hydration products have higher bulk density more than that of limestone. The bulk density of cement pastes decreases with limestone content due to the decrease of clinker content that decreases the amount of hydration products. The bulk density decreases whereas the total porosity increases with limestone content due to the decrease of OWPC.

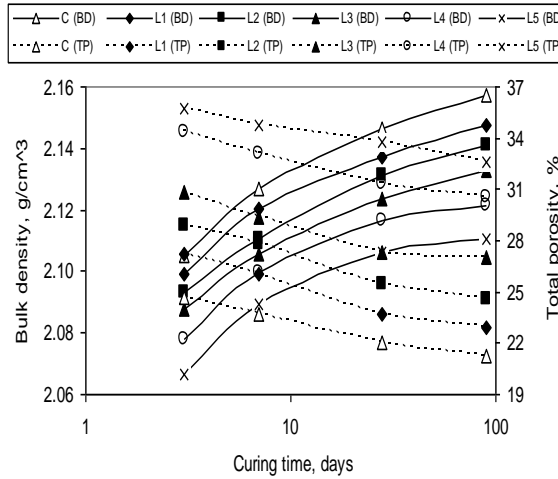


FIGURE (6): Bulk density and total porosity of OWPC and limestone blended cement pastes

7. Free Lime Content

Figure (7) illustrates the free lime content of OWPC and limestone blended cement pastes. The free lime content increases with curing time and limestone content. The increase of portlandite with curing time is due to the continuous liberation of portlandite due to the hydration process of β -C2S and C3S. On the other hand, the increase of portlandite with limestone content may be also due to some leaching of Ca^{2+} from $CaCO_3$.

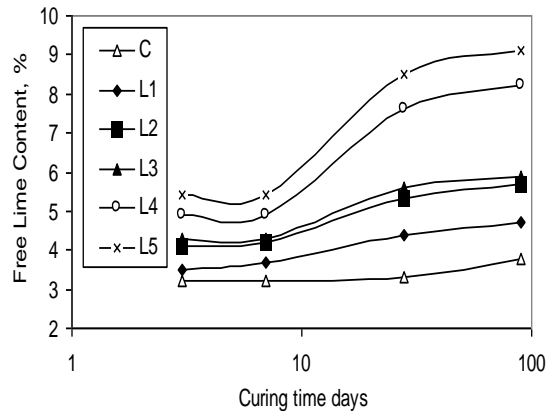


FIGURE (7): Free lime content of OWPC and limestone blended cement pastes

8. XRD Analysis

Figure (8) illustrates the XRD patterns of OWPC hydrated up to 90 days. It was observed that the content of portlandite increases with curing time as an indication to progress of hydration. On the other hand, there is no sign for the appearance of C-S-H except weak peak near 51.60 indicating that C-S-H has bad ordered structure. Dicalcium silicate C2S, still appear until reaching 90 days of hydration due to its slow rate of hydration. Calcite residue appears as an indication for partial carbonation of portlandite with atmospheric carbon dioxide and limestone as well as bicarbonate ions dissolved in mixing and curing water.

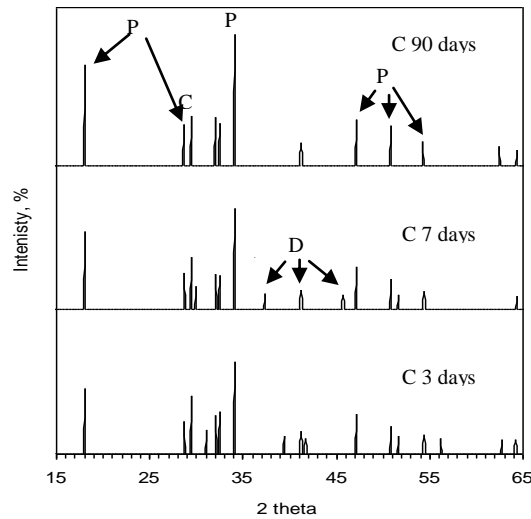


FIGURE (8): XRD patterns of OWPC hydrated up to 90 days where (P) portlandite, (C) calcite and (D) C₂S

Figure (9) illustrates XRD patterns of L4 hydrated up to 90 days. It was observed that tricalcium silicate C3S and dicalcium silicate C2S exist up to 7 days of hydration then disappeared at 90 days of hydration indicating that limestone acts as inert filler at early ages of hydration then accelerate the hydration of C3S at later ages of hydration. The portlandite increases with curing time up to 90 days due to the leaching of some Ca²⁺ from limestone in addition to its liberation due to hydration of OWPC.

Figure (10) illustrates XRD patterns of OWPC, L2, L4 and L5 hydrated for 7 days. It was observed that content of portlandite decreases as limestone content increases. This is because the filler effect of limestone. Small amount of limestone acts as nucleating agent which accelerates the rate of hydration and liberation of portlandite. On the other hand, the peak of portlandite decreases with limestone content.

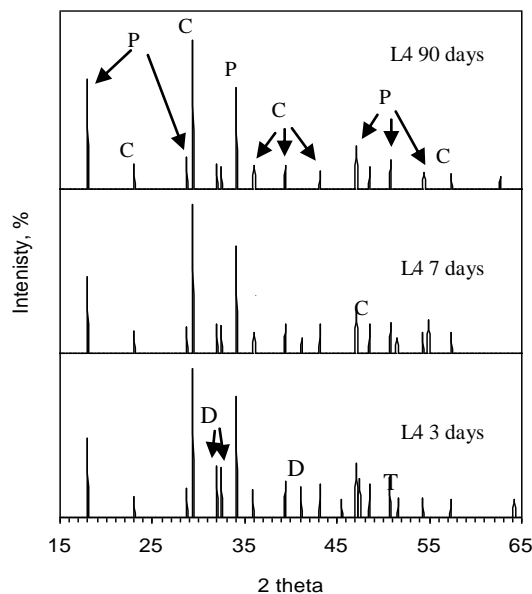


FIGURE (9): XRD patterns of L4 hydrated up to 90 days where (P) portlandite, (C) calcite, (D) C₂S and (T) C₃S

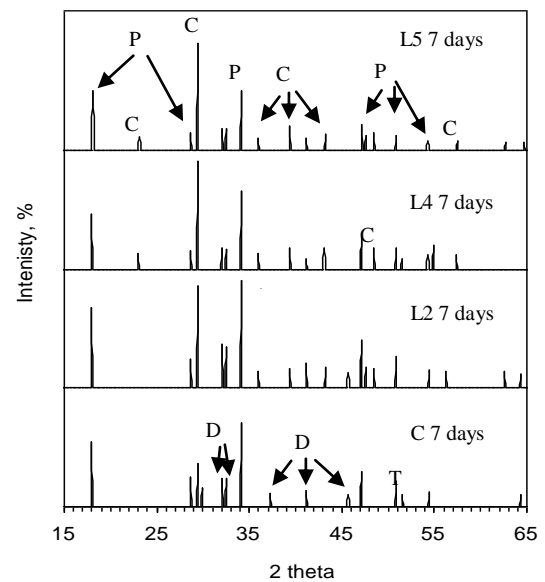


FIGURE (10): XRD patterns of OWPC, L2, L4 and L5 hydrated for 7 days where (P) portlandite, (C) calcite, (D) C₂S and (T) C₃S

9. FTIR Analysis

Figure (11) illustrates FTIR spectra of OPWC and L1-5 hydrated for 7 days. Portlandite gives rise to its absorption band at 3643 cm⁻¹ (vibrations of OH- group stretching vibration) [51]. Calcite gives its absorption bands at 2530, 1800, 1420 and 700 cm⁻¹ [52]. Calcium monocarboaluminate (3CaO.Al₂O₃.CaCO₃.11H₂O) bands at 3578 cm⁻¹ and 874 cm⁻¹ increases with CaCO₃ content. FTIR spectra analyses prove that the hydration products of C3A react with CaCO₃, giving calcium carboaluminate hydrate, and calcium monocarboaluminate is stable up to 28 days [53]. The ettringite band at 1124 cm⁻¹ due to ν₃ mode of SO₄²⁻ increases. This absorption band disappeared due to that SO₄²⁻ ions were probably replaced by CO₃²⁻ [53]. The OH- band of combined water, associates hexagonal hydrates and calcium hydroxide gives raise to its absorption band around 3450 cm⁻¹ [54]. In case of the blended cement pastes, this OH- band is shifted demonstrating the accelerating effect of CaCO₃ on C3S hydration and also, due to the formation of calcium carboaluminate hydrate (band at 3578 cm⁻¹). The high intensity of OH- band of calcium carboaluminate hydrates (at 3578 cm⁻¹) proves that calcium carboaluminate hydrates have higher water content than C-S-H [6 and 55]. Tobermorite, C-S-H gives raise to its absorption band at 978 cm⁻¹ (stretching vibration ν₃ of SiO₄⁴⁻) [55].

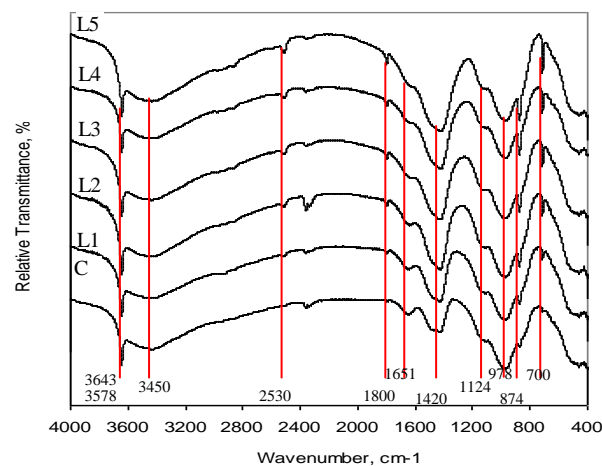


FIGURE (11): FTIR spectra of OPWC, L1-L5 hydrated for 7 days

Figure (12) illustrates FTIR spectra of L4 hydrated up to 90 days. Portlandite gives raise to its absorption band at 3643 cm⁻¹ (vibrations of OH- group stretching vibration). Calcite gives its absorption bands at 2530, 1800, 1420 and 700 cm⁻¹. Calcium monocarboaluminate (3CaO.Al₂O₃.CaCO₃.11H₂O) gives raise to its absorption bands at 3578 cm⁻¹ and 874 cm⁻¹. The calcium monocarboaluminate phase is a more stable product due to its greater insolubility [56] at ambient temperature and this is probably the reason for which the calcium monocarboaluminate is observed as main hydration product at early age [57]. Ettringite gives raise to its absorption band at 1124 cm⁻¹ due to ν₃ mode of SO₄²⁻. This absorption band disappeared due to that SO₄²⁻ ions were probably replaced by CO₃²⁻. The OH- band around 3450 cm⁻¹ of combined water, associates hexagonal hydrates and calcium hydroxide increases.

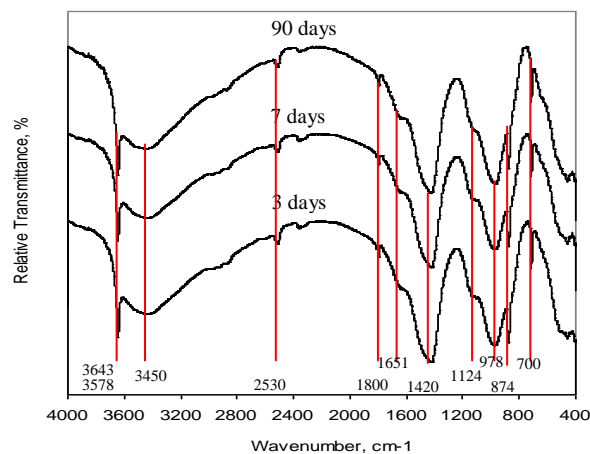


FIGURE (12): FTIR spectra of OPWC, L1-L5 hydrated for 7 days

10. SEM Micrographs

Figure (13) illustrates SEM micrographs of OWPC and L1-5 hydrated for 7 days. It was observed that the morphology of limestone blended cement pastes differs than that of OWPC. This can be attributed to the formation of calcium monocarboaluminate as a result of reaction of calcium carbonate with tricalcium aluminate.

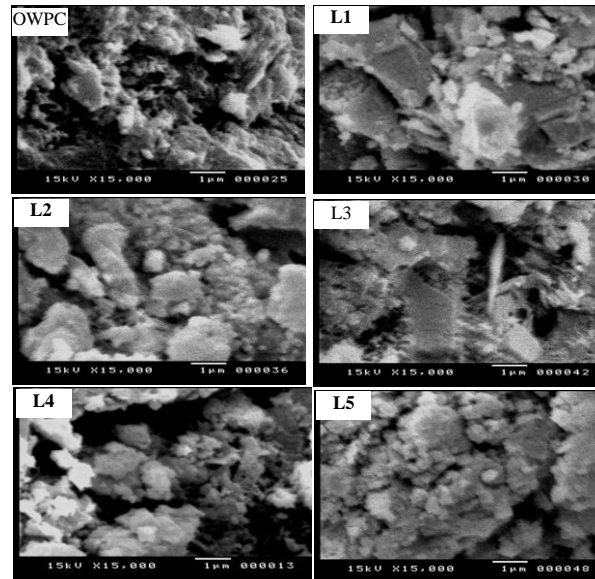


FIGURE (13): SEM micrographs of OWPC, L1-L5 hydrated for 7 days

Figure (14) illustrates SEM micrographs of L4 hydrated up to 90 days. It can be observed that the morphology of main hydration product that appear in limestone blended cement pastes i.e., calcium monocarboaluminate, originally changes with progress of hydration age. Such phenomenon has been observed and discussed in previous a work [58], where the investigator observed that calcium monocarboaluminate originally appears with irregular long thick shape and then changes to long rod shape at the hydration age of 3 days, and finally changes to fine-needle appearance at hydrate age of 90 days.

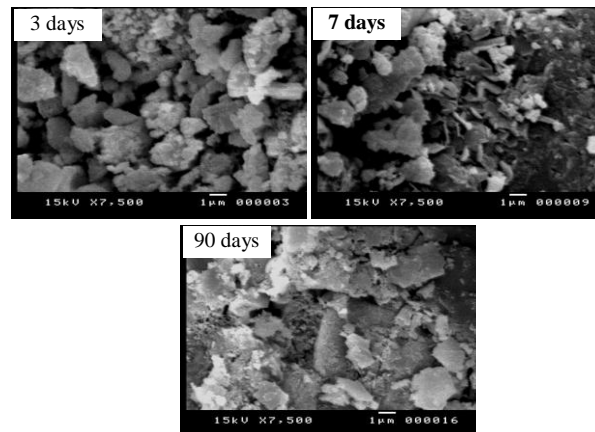


FIGURE (14): SEM micrographs of L4 hydrated for 3, 7 and 90 days.

11. TGA/DTA Thermograms

Figure (15) illustrates the TGA/DTA thermograms of OWPC and L4 hydrated for 90 days. Result of thermal analysis were illustrated in tables (4 and 5). The TGA/DTA thermograms illustrate the presence of three decomposition steps that occur at the temperature ranges 29-311, 311-582 and 582-1000 oC respectively. Evaporation of free water and dehydration of tobermorite gel, C-S-H and ettringite ($3\text{CaO}\cdot\text{Al}_2\text{O}_3\cdot 3\text{CaSO}_4\cdot 3\text{H}_2\text{O}$)

occur at the temperature range, 29-311 oC [59]. Portlandite, Ca(OH)_2 dehydrates at the temperature range, 390-582 oC [60]. Dehydration of dihydrated calcium sulfate (gypsum) mainly occurs up to 400-450 oC [61]. Finally, calcite decomposes at temperature range, 582-1000 oC [62].

From the result of thermal analysis illustrated in Tables (4 and 5), it was observed that the weight losses of OWPC occur at the temperature ranges 29-311 and 390-582 °C are higher than those of L4 blended cement paste hydrated for 90 days. This is due to the dilution effect of limestone that replaces 20% of OWPC. In contrast, it was observed that the weight loss of OWPC occur at the temperature range 582-1000 °C is lower than of L4 blended cement paste hydrated for 90 days. This is due to that L4 blended cement paste contains

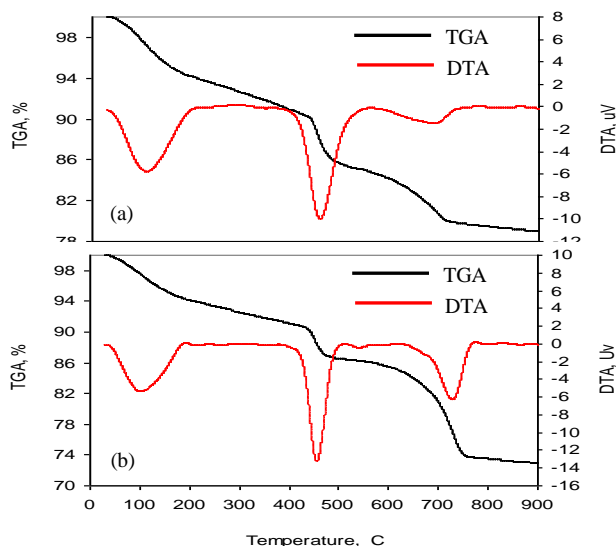


FIGURE (15): TGA and DTA thermograms of (a) OWPC and (b) L4 hydrated for 90 days

TABEL (4): RESULT OF THERMAL ANALYSIS HYDRATED FOR 90 DAYS

OWPC					
No.	Phase Changes	Tem °C	Peak Tem °C	Weight Loss %	Weight Loss mg
1	Dehydration of portlandite and gypsum	29-390	96	-7.61	-1.40
2	Decomposition of C-S-H	390-582	452	-7.94	-1.44
3	Decomposition of calcite	582-1000	698	-5.52	-1.00
Total				-21.07	-3.84

L4					
No.	Phase Changes	Temp °C	Peak Tem. °C	Weight Loss %	Weight Loss mg
1	Dehydration of portlandite and gypsum	31-252	100	-6.64	-1.24
2	Decomposition of C-S-H	252-575	452	-7.40	-1.39
3	Decomposition of calcite	572-1000	730	-13.04	-2.44
Total				-27.08	-5.07

Conclusions

- [1] Limestone filler increases whiteness, Blaine, free lime content and loss on ignition of dry blended cement powders due to the high whiteness, Blaine and loss on ignition of limestone compared to clinker.
- [2] Limestone filler increases setting times and total porosity of cement pastes. Limestone filler decreases compressive strength, combined water content and bulk density of cement pastes due to the filling effect of limestone that replaces clinker and decreases the amount of hydration products.
- [3] Portlandite was detected in limestone blended cement pastes hydrated for 7 days by XRD indicating the filler effect of limestone at early ages of hydration. Whereas, C₂S was not detected in limestone blended cement pastes hydrated up to 90 days by XRD indicating that limestone filler accelerates the rate of hydration of C₃S at later ages of hydration.

- [4] Calcium monocarboaluminate was detected in limestone blended cement pastes hydrated for 7 days by FTIR indicating that C3A reacts with CaCO_3 giving calcium monocarboaluminate. The absorption band of ettringite disappeared due to that SO_4^{2-} ions were probably replaced by CO_3^{2-} .
- [5] The OH⁻ band of combined water, associates hexagonal hydrates and calcium hydroxide was shifted in FTIR spectra of limestone blended cement pastes, demonstrating the accelerating effect of CaCO_3 on C3S hydration and formation of calcium carboaluminate hydrate.
- [6] Relative weight losses are useful for characterizing these materials. Weight losses that correspond to dehydration of C-S-H, ettringite and portlandite (calculated from TGA/DTA thermograms) prove the dilution effect of limestone filler.
- [7] SEM micrographs of limestone blended cement pastes hydrated up to 90 days detected that limestone filler alter the microstructure of hardened cement pastes. The morphology of calcium monocarboaluminate originally changes with progress of hydration.

References

- [1] H.H.M. Darweesh, *Ceramics International* 30 (2004), 145–150.
- [2] V.B. Bosiljkov, *Cement and Concrete Res.* 33 (2003), 1279–1286.
- [3] S. Tsvivilis, E. Chaniotakis, E. Badogiannis, G. Pahoulasa, A. Ilias, *Cement and Concrete Composites* 21 (1999), 107–116.
- [4] M. Heikal, H. El-Didamony, M.S. Morsy, *Cement and Concrete Res.* 30 (2000), 1827–1834.
- [5] H. El-Didamony, T. Salem, N. Gabr, T. Mohamed, *Ceram-Silik* 39 (1995), 15± 19.
- [6] J. Pera, S. Husson, B. Guilhot, *Cem. Concr. Compos.* 21 (1999), 99–105.
- [7] G. Menendez, V. Bonavetti, E.F. Irassar, *Cement & Concrete Composites* 25 (2003) 61–67.
- [8] P. Poitevin, *Cem. Concr. Comp.*, 21 (1999), 89–97.
- [9] M. Nehdi, S. Mindess, P.C. Aitcin, *Cement and Concrete Research*, Vol. 28, No. 5 (1998), pp. 687–697.
- [10] P. Hawkins, P. Tennis, R. Detwiler, Portland Cement Association, (2003), Report n. EB227.
- [11] V.L. Bonavetti, V.F. Rahhal, E.F. Irassar, *Cem. Concr. Res.* 31 (6) (2001), 853– 859.
- [12] A. Notat, *Mat. Struct.* 27 (168) (1994), 187–195.
- [13] V. Bonavetti. MSc thesis, Argentine, University of Center Buenos Aires State, (1998).
- [14] V. Bonavetti, H. Donza, V. Rahhal, E. Irassar, *Cem. Concr. Res.* 30 (5) (2000), 703– 708.
- [15] M. Bédérina, M.M. Khenfer, R.M. Dheilly, M. Quéneudec, *Cem. Concr. Res.* 35 (2005), 1172–1179.
- [16] H. Uchikawa, S. Hanehara, H. Hirao, *Cem. Concr. Res.* 26 (1) (1996), 101–111.
- [17] S.K. Agarwal, D. Gulati, *Cons. Build. Mat.* 20 (2006), 999–1004.
- [18] P. Lawrence, M. Cyr, E. Ringot, *Cem. Concr. Res.* 35 (2005), 1092–1105.
- [19] S.A. Hartshorn, J.H. Sharp, R.N. Swamy. *Cem Concr Res* (1999),29(8): 1331–40.
- [20] S.A. Hartshorn, R.N. Swamy, J.H. Sharp. *Adv Cem Res* (2001), 13(1):31–46.
- [21] M.A. Helal, *Cement and Concrete Research* 32 (2002), 447–450.
- [22] A.M. Poppe, G. Schutter, *Cement and Concrete Research* 35 (2005), 2290 – 2299.
- [23] B. Lothenbach, G. Saout, E. Gallucci, K. Scrivener, *Cement and Concrete Res.* 38 (2008), 848–860.
- [24] T. Matschei, B. Lothenbach, F.P. Glasser, *Cement and Concrete Res.* 37 (2007), 551–558.
- [25] M. Nehdi, *Cem. Concr. Res.* 30 (10) (2000), 1663– 1669.
- [26] A. Ghezal, K.H. Khayat, *ACI Mater. J.* 99 (3) (2002), 264– 272.
- [27] P. Billberg, *Cachan Cedex*, (1999), pp. 591– 602.
- [28] Y. Benachour, C.A. Davy, F. Skoczylas, H. Houari, *Cement and Concrete Res.* 38 (2008), 727–736.
- [29] X. Zhang, J. Han, *Cement and Concrete Research* 30 (2000), 827±830.
- [30] P. Ballester, I. Mármol, J. Morales, L. Sánchez, *Cement and Concrete Res.* 37 (2007), 559–564.
- [31] B.S. Hamad, *Advanced Cement Based Materials*, (1995), 2:161-167.
- [32] H.F.W. Taylor, *Cement Chemistry*, 2nd edition, Thomas Telford, London, (1997).
- [33] J. Skibsted, H.J. Jakobsen, C. Hall, *J. Chem. Soc., Faraday Trans.* 90 (1994), 2095–2098.
- [34] I.G. Richardson, A.R. Brough, R. Brydson, G.W. Groves, C.M. Dobson and EELS, *J. Am. Ceram. Soc.* 76 (1993), 2285– 2288.
- [35] M.D. Andersen, H.J. Jakobsen, J. Skibsted, *Inorg. Chem.* 42 (2003), 2280–2287.
- [36] H. Stade, D. Muller, *Cem. Concr. Res.* 17 (1987), 553– 561.
- [37] D.S. Klimesch, A.S. Ray, *Adv. Cem. Res.* 11 (1999), 179– 187.
- [38] P. Faucon, A. Delagrave, J.C. Petit, C. Richet, J.M. Marchand, H. Zanni, *J. Phys. Chem., B* 103 (1999), 7796–7802.

- [39] J. Hjorth, J. Skibsted, H.J. Jakobsen, *Cem. Concr. Res.* 18 (1988), 789–798.
- [40] S. Martinez-Ramirez and M. Frias, *Construction and Building Materials* 23 (2009), 1344–1348.
- [41] C.A. Love, I.G. Richardson, A.R. Brough, *Cement and Concrete Res.* 37 (2007), 109–117.
- [42] A.V. Girão, I.G. Richardson, C.B. Porteneuve, R.M.D. Brydson, *Cement and Concrete Res.* 37 (2007), 1571–1582.
- [43] J. Xiao, C.F. Gou, Y.G. Jin, Y.H. Wang, *J. Cent. South Univ. Technol.* 17 (2010), 918–923.
- [44] ASTM designation: C 187-98. *Annual Book of ASTM Standards*, (2002), 04.01.
- [45] ASTM designation: C 191-01a. *Annual Book of ASTM Standards*, (2002) 04.01.
- [46] Gennaro R, Cappelletti P, Cerri G, Gennaro M, Dondi *Appl Clay Sci* (2004), 25:71.
- [47] ASTM designation: C109-80. *Annual Book of ASTM Standards*; (1983).
- [48] J. Pavlik, V. Tydlitát, R. Cerný, T. Klecka, P. Bouska, P. Rovnanikova. *Cem Concr Res* (2003), 33:93.
- [49] L.E. Copeland, T.C. Hayes, Porosity of hardened Portland cement pastes. *ACI Mater* (1956), 27:633.
- [50] R. Kondo, S.A. Abo-El-Enein, M. Daimon, *Bull Chem Soc Jpn* 48 (1975), 222-226.
- [51] F.A. Rodrigues, American Chemical Society, New Orleans, 39 (2) (1999), 30-31.
- [52] H. Boke, O. Cizer, B. Ipekoglu, E. Ugurlu, K. Serifaki, G. Toprak, *Const. Build.*, 22 (2008), 866-874.
- [53] D. Govindarajan1, R. Gopalakrishnan, *Frontiers in Science* (2011), 1(1): 21-27.
- [54] T. El-Sokkary, M. Saraya, M.A. Tantawy, M.A. Taher, *HBRC journal* 6 (2) (2010), 36-45
- [55] M.A. Trezza, A.E. Lavat, *Cem. Concr Res.*, 31 (2001), 869-872.
- [56] W. Klemm, L. Adams, *ASTM Specifications Technology Publication*, 1064, (1990), 60-72.
- [57] J. Bensted, *World cement technology*, 11 (8) (1980), 395-406.
- [58] J. Dweck, P.M. Buchler, A.C.V. Coelho, F.K. Cartledge, *Thermochimica Acta* 346 (2000), 105-113.
- [59] J. Dweck, P. Souza Santos, *Ceraâmica* 37(250) (1991), 80.
- [60] J. Dweck, E.I.P. Lasota, *Thermochim. Acta* 318 (1998), 137.
- [61] A. Bakolas, G. Biscontin, A. Moropoulou, E. Zendri, *Thermochim. Acta* 321 (1998), 151–160.
- [62] J. Adams, D. Dollimore, D.L. Griffiths, *Thermochim. Acta* 324 (1998), 67–76.